Talanta 104 (2013) 149–154

Contents lists available at SciVerse ScienceDirect

Talanta

journal homepage: www.elsevier.com/locate/talanta

Biosensor based on hydrogel optical waveguide spectroscopy for the detection of 17β-estradiol

Qingwen Zhang [a,b], Yi Wang [b,c,**], Anca Mateescu [d], Khulan Sergelen [b], Asmorom Kibrom [b], Ulrich Jonas [d,e], Tianxin Wei [a], Jakub Dostalek [b,*]

[a] Key Laboratory of Cluster Science of Ministry of Education, Beijing Institute of Technology, Beijing 100081, China
[b] Austrian Institute of Technology GmbH, Biosensor Technologies, Muthgasse 11, Vienna 1190, Austria
[c] Nanyang Technological University, Centre for Biomimetic Sensor Science, 637553 Singapore, Singapore
[d] Foundation for Research and Technology Hellas (FORTH), Bio-Organic Materials Chemistry Laboratory (BOMCLab), P.O. Box 1527, 71110 Heraklion, Crete, Greece
[e] Macromolecular Chemistry, University of Siegen, Department Chemistry – Biology, Adolf-Reichwein-Strasse 2, Siegen 57076, Germany

ARTICLE INFO

Article history:
Received 11 May 2012
Received in revised form
6 November 2012
Accepted 9 November 2012
Available online 21 November 2012

Keywords:
Surface plasmon resonance (SPR)
Hydrogel optical waveguide (HOW)
Hydrogel binding matrix
17β-estradiol (E2)
Biosensors

ABSTRACT

Rapid detection of hormones at sub-ng/ml concentrations is of tremendous importance for diagnostic purposes, quality control, and environmental monitoring. In this respect, we report a novel label-free biosensor based on hydrogel optical waveguide spectroscopy (HOWS) for the sensitive detection of 17β-estradiol (E2). This approach was implemented by using a thin hydrogel layer of a carboxylated poly(*N*-isopropylacrylamide) (PNIPAAm) terpolymer that was attached to a metallic sensor surface in order to simultaneously serve as a binding matrix and an optical waveguide. Refractive index changes that are accompanied with the specific capture of biomolecules from an aqueous sample on the sensor surface were probed by resonantly excited hydrogel optical waveguide modes. To optically excite and interrogate these waves, an optical setup based on Kretschmann configuration of attenuated total reflection (ATR) method that is compatible with surface plasmon resonance (SPR) was used. We demonstrate that HOWS offers a higher binding capacity, good anti-fouling properties, improved figure of merit, and E2 detection limit of 50 pg/ml which is seven times better than that obtained by a regular surface plasmon resonance (SPR) biosensor.

© 2012 Elsevier B.V. All rights reserved.

1. Introduction

Surface plasmon resonance (SPR) is an optical phenomenon which originates from coupled oscillations of charge density and electromagnetic field intensity on a metallic surface and it received great deal of attention for sensor applications [1–3]. SPR is sensitive to refractive index changes occurring upon the binding of molecules to a metallic surface which provides an attractive means for direct, rapid, and sensitive detection of molecular analytes. The key advantage of this optical technique is its ability to directly monitor a specific capture of target molecules from a sample on the sensor surface without the need of additional labels. SPR biosensors were shown to be suitable for the analysis of medium or large molecular weight analytes which induce measurable refractive index changes upon their binding on the surface from samples with the analyte concentrations above ng/ml [4]. However, for many application in important fields of medical diagnostics, food control, and environment monitoring [5–8], this sensitivity is not sufficient.

In order to advance the sensitivity of SPR-based biosensors, carboxylated photocrosslinkable hydrogel polymer networks [9,10] were attached to a metallic sensor surface and employed as a large binding capacity matrix [11,12] in our laboratory. These highly swollen materials with a thickness up to several micrometers were shown to accommodate more than an order of magnitude larger amount of biomolecular recognition elements compared to conventional monolayer-based surface architectures. Moreover, such hydrogel films can serve as a waveguide that supports additional waves propagating along the sensor surface with lower losses than surface plasmons employed in regular SPR biosensors. This feature allows increasing the figure of merit (FOM) and resolution in the measurement of analyte binding-induced refractive index changes by using the hydrogel optical waveguide spectroscopy (HOWS) [12]. A model immunoassay experiment showed that the HOWS can advance the limit of detection for large molecular weight biomolecules

* Corresponding author at: Austrian Institute of Technology GmbH, Biosensor Technologies, Muthgasse 11, Vienna 1190, Austria. Tel.: +43 50550447; fax: +4 350 550 4399.
** Corresponding author at: Nanyang Technological University, Centre for Biomimetic Sensor Science, Singapore 637553, Singapore. Tel.: +65 65927948.
E-mail addresses: yiwang@ntu.edu.sg (Y. Wang), jakub.dostalek@ait.ac.at (J. Dostalek).

0039-9140/$ - see front matter © 2012 Elsevier B.V. All rights reserved.
http://dx.doi.org/10.1016/j.talanta.2012.11.017

such as immunoglobulin G by a factor of 5 with respect to regular SPR [12].

In this work, we report an implementation of HOWS for detection of a low molecular weight analyte—17β-estradiol (E2). E2 is a natural estrogen hormone, which occurs at levels in the range from pg/ml to ng/ml in blood and urine depending on the phase of menstrual cycle of adult females [13,14]. Assays for the analysis of E2 are important for clinical endocrinological investigations of menstrual disorder, hormonal infertility treatment, evaluating ovarian function, and tumor diagnosis [15,16]. In addition, it has been reported that E2 can enter into the human body from the outer environment and interfere with normal physiological processes [17,18]. Therefore, the monitoring of E2 in environmental or waste water is an important issue [18–20]. A great variety of methods for the analysis of E2 has been developed exploiting fluorescence immunoassays [21,22], chemiluminescence immunoassays [14,18,23], radioimmunoassay [24,25], homogenous noncompetitive immunoassay [26,27], as well as gas chromatography-mass spectrometry (GC–MS) [28]. These detection methods typically offer sufficient limit of detection (LOD), however, they are laboratory-based, rely on complex instrumentation, and are time-consuming. In this paper, we address the need for new tools enabling simpler and faster analysis of E2 and report a new inhibition immunoassay-based biosensor relying on hydrogel optical waveguide spectroscopy which is compatible with SPR biosensor instrumentation and provides an improved sensitivity.

2. Experimental section

2.1. Materials

All reagents were used as received without further purification. E2 (Catalog No. E8875) and the conjugate of E2 with bovine serum albumin (BSA-E2, Catalog No. E5630) were purchased from Sigma–Aldrich (Germany). Mouse monoclonal antibody to E2 (anti-E2 antibody, Catalog No. E86022M) was obtained from Meridian Life Science (USA). 1-ethyl-3-(3-dimethylaminopropyl)-carbodiimide hydrochloride (EDC) and *N*-hydroxysuccinimide (NHS) were obtained from Pierce (USA). Phosphate buffered saline (PBS, 140 mM NaCl, 10 mM phosphate, 3 mM KCl, and pH 7.4) was purchased from Calbiochem (Germany). 10 mM acetate buffer (ACT, pH 4) was prepared from sodium acetate and acetic acid and the pH was adjusted by HCl and NaOH. PBS Tween (PBST) buffer was prepared by adding Tween 20 (0.05%) to PBS buffer solution. Dithiolalkanearomatic PEG6-carboxylate (thiol-COOH, Catalog No. SPT-0014A6) and dithiolalkanearomatic PEG3 (thiol-PEG, Catalog No. SPT-0013) were purchased from SensoPath Technologies (USA). Sodium para-tetrafluorophenol-sulfonate (TFPS) [29] and 3-(4-benzoylphenoxy)propanethiol (thiol-benzophenone) [30] were synthesized in our laboratory as described in literature. Glycine buffer with pH 1.5 and ethanolamine were purchased from Biacore (Germany). Artificial urine samples (AU) with pH 6.5 were prepared by dissolving 133 mM sodium chloride, 58 mM potassium chloride, 290 mM urea, 10 mM sodium phosphate, 28 mM creatinine (from Sigma–Aldrich C4255), and 30 μg/ml of human serum albumin (HSA, from Sigma Aldrich, A8763) in water [31]. Human serum samples were obtained from freshly drawn blood incubated at room temperature for 30 min followed by the centrifugation at 2000 rpm for 15 min. The human serum samples were stored at −80 °C prior to the use.

2.2. Sensor surface functionalization

Poly(*N*-isoproprylacrylamide) – based hydrogel (PNIPAAm) was synthesized by free radical polymerization as described in elsewhere [32]. A random terpolymer was composed of (NIPAAm, 94% monomer concentration), methacrylic acid (MAA, 5% m.c.), and 4-benzophenonemethacrylate (BPMA, 1% m.c.). PNIPAAm-based hydrogel was dissolved in ethanol at the concentration of 20 mg/ml and spincoated on a gold surface that was modified with a thiol-benzophenone self-assembled monolayer (SAM). The thiol-benzophenone SAM was formed on the gold surface upon overnight incubation in ethanol solution with 1 mM thiol-benzophenon followed by the rinsing with pure ethanol and drying with a stream of nitrogen.The PNIPAAm film was subsequently dried overnight in vacuum at 50 °C, simultaneously cross-linked and anchored to the gold surface by UV light (λ=365 nm, irradiation dose of 2 J/cm^2), and the crosslinked three-dimensional polymer network was rinsed with water and dried in a stream of nitrogen. BSA-E2 conjugates were immobilized in the PNIPAAm hydrogel via their amine groups. Firstly, the carboxylic acid groups in the PNIPAAm hydrogel were activated by its immersing in a water solution with a mixture of TFPS (10.5 mg/ml) and EDC (37.5 mg/ml) for about 1 h followed by the rinsing with water and drying in a stream of nitrogen. Afterwards, the BSA-E2 conjugate dissolved in ACT at a concentration of 1 mg/ml was overnight reacted with active ester moieties in the PNIPAAm hydrogel at 4 °C. Finally, the sensor surface was rinsed with water and dried under a stream of nitrogen. The overall scheme of the PNIPAAm three-dimensional binding matrix can be seen in Fig. 1a. For comparison, regular two-dimensional surface architecture was used for the modification of gold surface based on a mixed thiol SAM, see Fig. 1b. Firstly, the gold surface was incubated overnight in a mixture of thiol-PEG and thiol-COOH (molar ratio of 9:1) dissolved in ethanol at the total concentration of 1 mM in order to form a SAM. Afterwards, the surface was rinsed with ethanol and dried in a stream of nitrogen. The carboxylic moities on the mixed thiol SAM surface were activated with EDC (37.5 mg/ml) and NHS (10.5 mg/ml) dissolved in an aqueous solution followed by the covalent coupling of BSA-E2 conjugates. The unreacted carboxylic groups on the mixed thiol SAM and in the NIPAAm-based hydrogel binding matrix were blocked by 20 min incubation with 1 M ethanolamine at pH 8.5.

2.3. Sensor implementation

An optical setup utilizing angular spectroscopy of surface plasmons (SP) and hydrogel optical waveguide (HOW) waves was used as described in our previous reports [11,12]. Briefly, a transverse magnetically (TM) polarized beam from a HeNe laser (2 mW, λ=632.8 nm) was coupled to a 90° LASFN9 glass prism and reflected from the prism base at the angle of incidence θ. To the prism base, a sensor chip was optically matched by using an immersion oil. The sensor chip consisted of a BK7 glass substrate that was coated by sputtering (UNIVEX 450C from Leybold, Germany) with 45 nm thick gold film. On the gold surface, BSA-E2 conjugates were immobilized either by using a mixed thiol SAM (regular SPR sensor chip) or PNIPAAm hydrogel (HOWS sensor chip). A flow-cell with the volume of approximately 10 μl was pressed against the sensor surface in order to flow liquid samples at a flow rate of 500 μl/min. The analyzed sample with the volume of 800 μl was made circulating in the closed fluidic system. Let us note that the total volume of the fluidic system (and thus the volume of analyzed sample) can be reduced by taking advantage of more advanced microfluidics components. The excitation of SP and HOW waves by the laser beam hitting the gold layer was observed from the angular reflectivity spectra $R(\theta)$ measured by using a photodiode detector and a rotation stage. The resonant coupling to these waves is manifested as respective dips in the reflectivity spectrum $R(\theta)$. Refractive index changes occuring on the sensor chip surface due to binding of the biomolecules were evaluated from measured reflectivity spectra

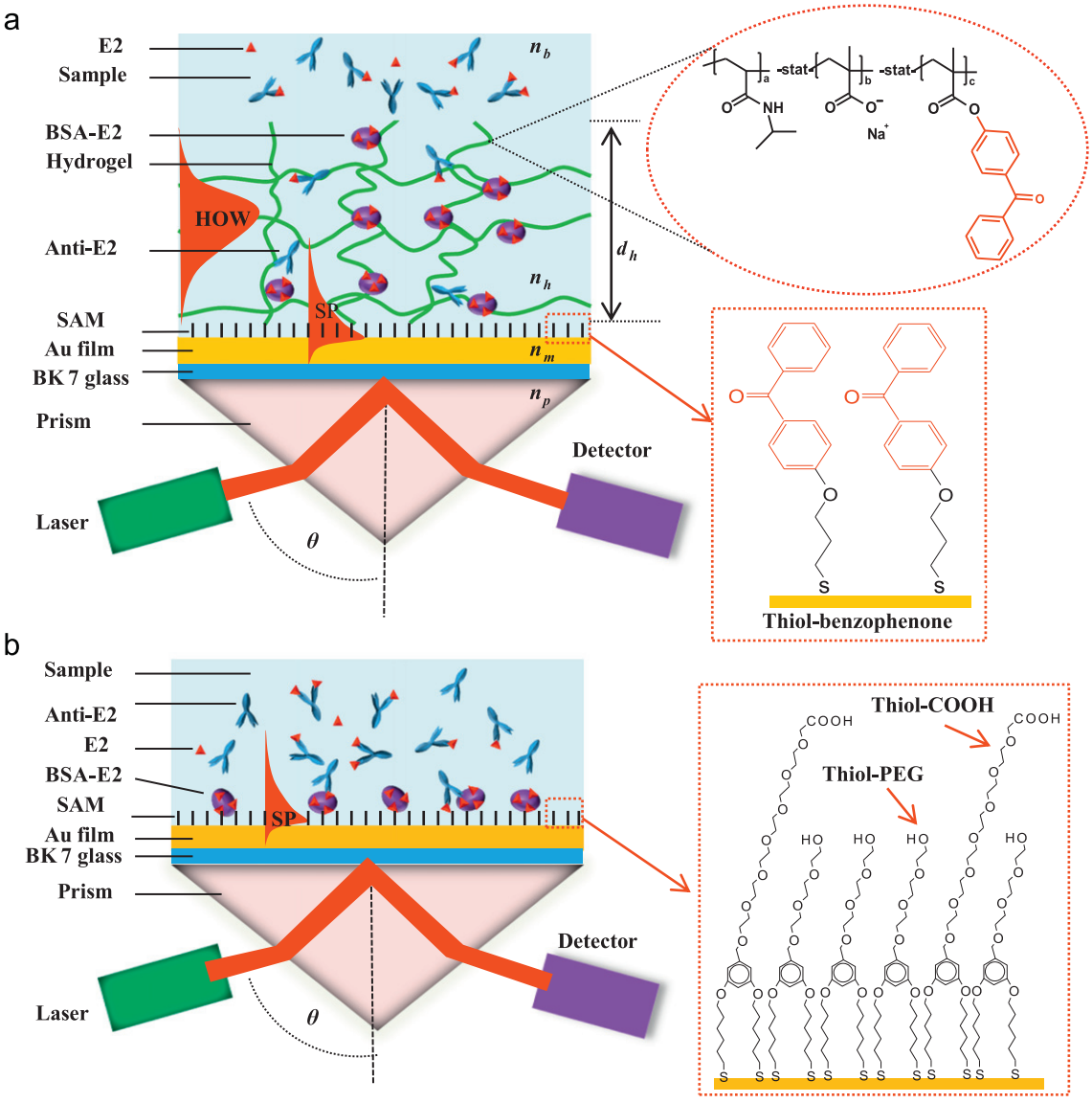

Fig. 1. The scheme of the optical setup and sensor chips with surface architectures supporting (a) HOW and (b) SP waves.

$R(\theta)$ by fitting with a transfer matrix-based model that was implemented in the software Winspall (developed at the Max Planck Institute for Polymer Research in Mainz, Germany). For HOWS sensor chips, this approach allowed for independent determining of both thickness d_h and refractive index n_h of the hydrogel film. Assuming that the refractive index of the gel n_h is uniform in the direction perpendicular to the surface (so called box model), these parameters can be used to determine the surface mass density of the polymer and immobilized biomolecules as

$$\Gamma = \frac{(n_h - n_b)d_h}{\partial n/\partial c} \quad (1)$$

where n_b is the refractive index of a buffer, in which the hydrogel is swollen. The factor of $\partial n/\partial c = 0.2\ \mathrm{mm^3/mg}$ that relates the refractive index changes with the concentration of PNIPAAm polymer chains and biomolecules was taken from the literature [33]. The polymer volume content f of the swollen hydrogel was calculated based on the effective medium theory as

$$f = \frac{(n_h^2 - n_b^2)(n_{h-dry}^2 + 2n_b^2)}{(n_h^2 + 2n_b^2)(n_{h-dry}^2 - n_b^2)} \quad (2)$$

where $n_{h-dry} = 1.5$ is the refractive index of the dry gel. For regular mixed thiol-based architecture, the surface mass density of a thin protein film Γ was calculated by using the same Eq. (1), in which the refractive index of a thin protein monolayer of $n_h = 1.5$ was assumed and the thickness d_h was obtained by fitting the respective SPR spectrum. The parameters used in the fitting of the reflectivity spectra $R(\theta)$ were as follows: refractive index of the prism $n_p = 1.845$, thickness of the gold film $d_m = 45.1$ nm, complex refractive index for the gold film $n_m = 0.22 + 3.67i$, and refractive index of the PBST buffer $n_b = 1.3337$.

2.4. Detection format

Inhibition immunoassay was used for the detection of E2 by using HOWS and regular SPR sensor chips. Samples were prepared by spiking the PBST buffer with E2 at concentrations ranging from 10^{-2} to 10^{3} ng/ml. Each sample was pre-incubated with anti-E2 at a concentration of 1 μg/ml for 20 min followed by the detection of unreacted anti-E2. Afterwards, the mixture of a sample and anti-E2 was pumped through the sensor for 15 min in order to let the free anti-E2 bind to the BSA-E2 conjugate on the mixed SAM (regular SPR readout) or in the PNIPAAm hydrogel (HOWS readout),

followed by rinsing of the sensor surface with PBST buffer for 3 min. After each detection cycle, the substrate surface was regenerated by rinsing with glycine buffer (pH 1.5, 20 mM) and sodium hydroxide (20 mM) for 2 min in order to release the anti-E2 from the surface.

3. Results and discussion

Firstly, the surface mass density of immobilized BSA-E2 and that of affinity bound anti-E2 was determined for two-dimensional mixed thiol SAM (regular SPR) and three-dimensional hydrogel bindng matrix (HOWS). As shown in Fig. 2, the reflectivity curves $R(\theta)$ were measured on a bare surface without BSA-E2 (1) and compared to those obtained after the immobilization of the BSA-E2 conjugate (2) and subsequent affinity binding of anti-E2 (3). On the regular SPR sensor chip prior to the modification, the resonant excitation of SPs occurs at $\theta=56.4^\circ$. The resonance shifts to higher angles θ after the binding of biomolecules to the surface due to the increase in thickness of the adlayer (Fig. 2b). From the measured resonance shift $\Delta\theta=0.40^\circ$, the surface mass density of covalently bound BSA-E2 was estimated as $\Gamma=1.8$ ng/mm^2. After affinity binding of anti-E2 from the PBST solution with the concentration of 10 μg/ml, additional shift of $\Delta\theta=0.37^\circ$ was observed which

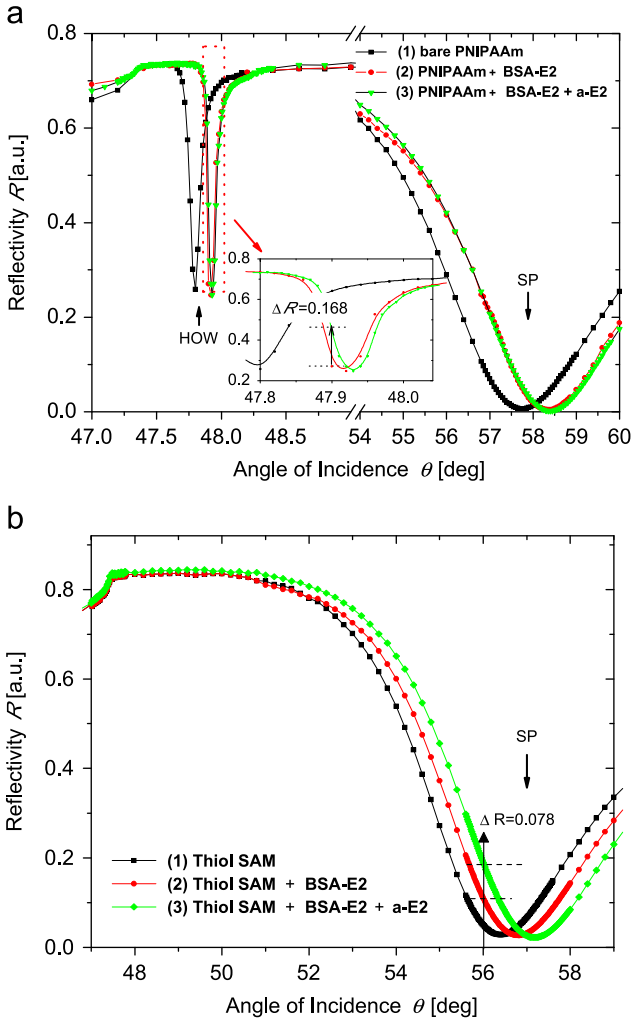

Fig. 2. Angular reflectivity spectra measured from a sensor chip carrying (a) a thin hydrogel film and (b) thiol SAM prior to the modification (1), after the immobilization of the BSA-E2 conjugate (2), and after the affinity binding of anti-E2 (3). The spectra were measured for surfaces brought in contact with PBST.

corresponds to the surface mass density of bound anti-E2 antibody of $\Gamma=1.7$ ng/mm^2. The kinetics measurement (data not shown) revealed that the binding reached saturation after 30 min flow of anti-E2. Taking into account the molecular weight of anti-E2 (~150 kDa) and the BSA-E2 conjugate (~75 kDa), from these data follows that ~50% of the BSA-E2 conjugates were accessible for the binding of anti-E2 on a the densely packed two-dimensional monolayer architecture.

For the sensor chip with three-dimensional hydrogel binding matrix, the reflectivity spectra in Fig. 2a show two distict resonances that are associated with the excitation of HOW and SP waves at angles of $\theta=47.8$ and 57.8°, respectively. Let us note that the coupling to the HOW mode occurs within an angular range (full width at half minimum – FWHM of 0.05°) which is more than 60 times narrower than that for regular SPR (FWHM$=3^\circ$). Similarly to SPR, HOW resonance shifts to higher angles after the covalent coupling of BSA-E2 ($\Delta\theta=0.13^\circ$) and after the affinity binding of anti-E2 ($\Delta\theta=0.016^\circ$). The analysis of the reflectivity curves in Fig. 2a showed that the bare hydrogel film exhibited the thickness of $d_h=1709$ nm and refractive index of $n_h=1.3468$. These data correspond to a surface mass density of the hydrogel of $\Gamma=112$ ng/mm^2. In addition, the polymer volume content of $f=8\%$ (determined by using Eq. (2) reveals that the PNIMAAm hydrogel binding matrix exhibits a highly swollen and thus open structure. After the immobilization of BSA-E2 in the hydrogel, the surface mass density of the hydrogel increased to 130 ng/mm^2, indicating that the net surface mass density of coupled BSA-E2 was $\Gamma=18$ ng/mm^2. This value is 10 times higher than that for the SPR chip with the mixed thiol SAM architecture. The surface mass density of the affinity-captured anti-E2 antibody from a solution with the concentration of 10 μg/ml was estimated to be $\Delta\Gamma=2$ ng/mm^2. This value is comparable to that for the SAM surface and is much smaller than the surface mass density of the BSA-E2 conjugate immobilized in the hydrogel. This observation may be ascribed to a slow diffusion of the analyte through the PNIPAAm hydrogel binding matrix [12], which did not reach saturation after 30 min flow of the sample (data not shown).

In further experiments, the angle of incidence of the laser beam was fixed at the resonance edge with the highest slope $dR/d\theta$ and the sensor signal was obtained as a reflectivity change ΔR (see in Fig. 2). For HOWS and SPR sensor chips functionalized with the BSA-E2 conjugate, these angles were set as $\theta=47.9^\circ$ and $\theta=56^\circ$, respectively. Let us note that owing to the narrower width of HOW resonance, the sensor signal ΔR due to binding of anti-E2 is higher for the HOWS-based sensor compared to that for regular SPR sensor (e.g., for the anti-E2 concetration of 10 μg/ml the factor is about 2.2). For the detection of E2 by the inhibition assay, the anti-E2 concentration of 1 μg/ml was used for both HOWS and SPR sensor platforms. The time-dependent reflectivity changes ΔR were measured upon the affinity binding of anti-E2 antibody that was pre-incubated with the E2 analyte at concentrations between 10^{-2} and 10^3 ng/ml. As shown in Fig. 3, the binding of anti-E2 to the BSA-E2 conjugate is manifested as a gradual increase in the sensor signal ΔR. The magnitude of the sensor signal ΔR is inversely proportional to the concentration of E2. For instance, a reflectivity change of $\Delta R=0.02$ was measured by SPR in the absence of E2 analyte, which is about 4-fold higher than the reflectivity change of $\Delta R=0.005$ measured in the presence of E2 with a concentration of 10^3 ng/ml (Fig. 3b). Compared to the SPR response, the HOWS signal shows a 1.75-fold higher maximum reflectivity change ΔR_0 in the absence of E2. The background signal measurements were carried out for the solution with 1 μg/ml anti-E2, which flowed over the SPR and HOWS sensor surface that was not modified with BSA-E2. The results in Fig. 3 indicate that the nonspecific binding of the antibody on the bare mixed thiol SAM and in the bare hydrogel

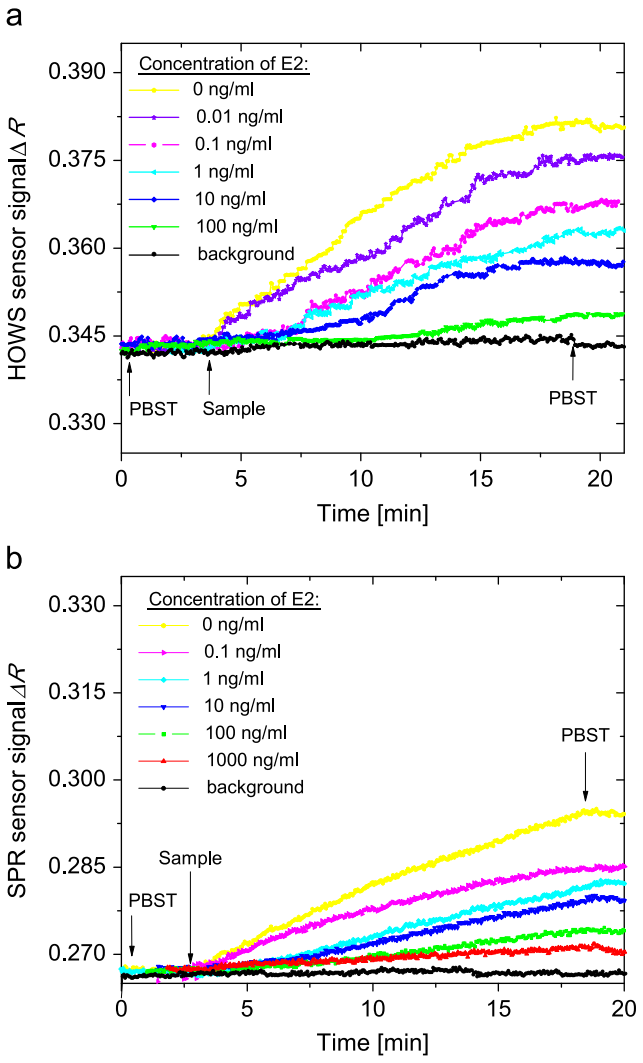

Fig. 3. The kinetics of reflectivity changes measured by (a) HOWS and (b) SPR upon the affinity binding of anti-E2 (1 μg/ml) incubated with a PBST samples spiked with E2 at concentrations between 10^{-2} and 10^{3} ng/ml.

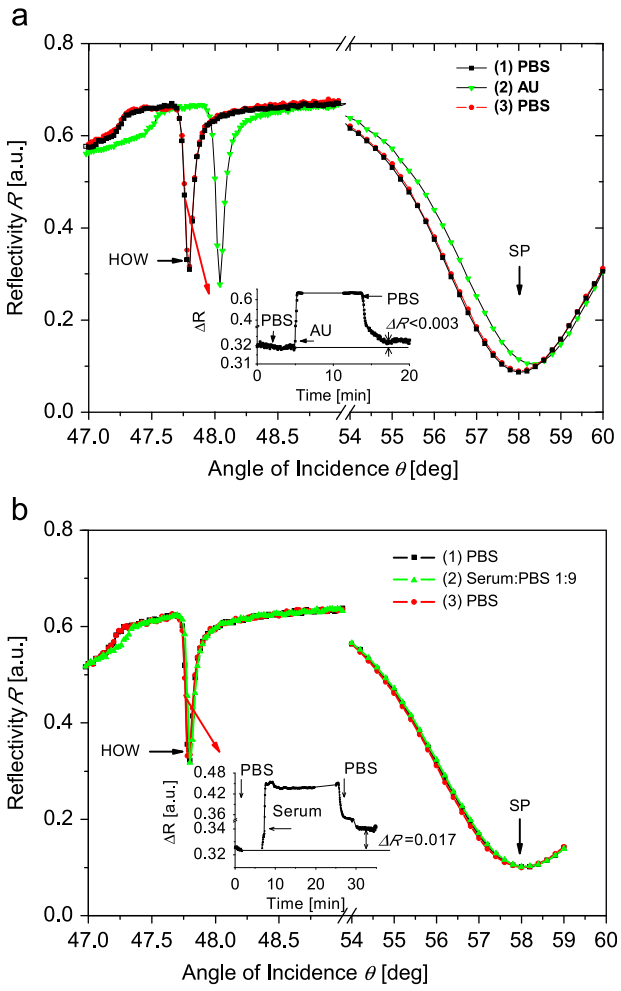

Fig. 4. Angular reflectivity measured by HOWS sensor carrying PNIPAAM hydrogel successively incubated in (a) PBS (1), artificial urine (2), and PBS (3) and (b) PBS (1), 10% serum (2), and PBS (3). The inset shows the respective kinetics of reflectivity signal measured at the angle of incidence $\theta = 47.7°$.

was negligible as relative reflectivity changes of $\Delta R/\Delta R_0 \sim 1\%$ and 3% were observed by SPR and HOWS, respectively.

The unspecific interaction of artificial urine (AU) and human serum with the PNIPAAm polymer networks was observed in order to evaluate the potential of HOWS for the analysis of E2 in these samples. Fig. 4 shows the reflectivity curves measured upon a successive incubation of the hydrogel surface with (a) PBS, AU, and PBS and (b) PBS, serum, and PBS. These data reveal that after the flow of AU, the resonance dips associated with the resonant excitation of HOW and SP waves shift to higher angles due to the increased refractive index of AU. However, the resonances shift to original values after the rinsing with PBS and no measurable changes in the surface mass density of PNIPAAm hydrogel were observed. The inset graph in Fig. 4a shows the respective kinetics of the reflectivity signal measured at the edge of the HOW resonance. The reflectivity change before and after the incubation with AU $\Delta R < 0.003$ is much smaller than that due to the affinity binding of anti-E2 antibody ($\Delta R = 0.160$ as seen in Fig. 2a). Compared to AU, the interaction with 10% human serum (diluted in PBS) is accompanied with significantly higher reflectivity change $\Delta R = 0.017$ (Fig. 4b) which is similar to the response measured for the anti-E2 binding (see Fig. 3a). The fact that both SP and HOW resonances shifted to higher angles after the flow of the serum indicates that the unspecific sorption occurred within the whole PNIPAAm network. Let us note that the NIPAAm polymer exhibits small negative net charge and that by applying a pH change the un-specifically adsorbed molecules were fully removed. These data indicate that the unspecific interaction with human serum would complicate the analysis of estradiol in this sample and that it can be eliminated by tuning the net charge of the polymer networks.

The HOWS and SPR biosensor calibration curves were normalized with the sensor response ΔR_0 measured in the absence of E2. As shown in Fig. 5, the sensor response ΔR was measured for each concentration in triplicate and the standard deviation σ is indicated as an error bar. The calibration curves were fitted with sigmoidal function and the limit of detection (LOD) was determined as the concentration of E2, for which the sensor response decreased by three times of the standard deviation of the reflectivity baseline that is normalized with the reflectivity change for a blank sample ($3\sigma/\Delta R_0 = 22.5\%$ for SPR and 17.7% for HOWS). The LOD of 50 pg/ml was determined for HOWS which is approximately 7-fold better than 0.34 ng/ml reached by regular SPR. This is partially due to the larger reflectivity changes associated with the binding of anti-E2 and associated lower relative standard deviation $\sigma/\Delta R_0$. In addition, one can see that the normalized sensor signal $\Delta R/\Delta R_0$ decreases faster with the E2 concentration for HOWS than for regular SPR. This effect further improves the LOD and we assume that it is due to easier accessibility of binding sites

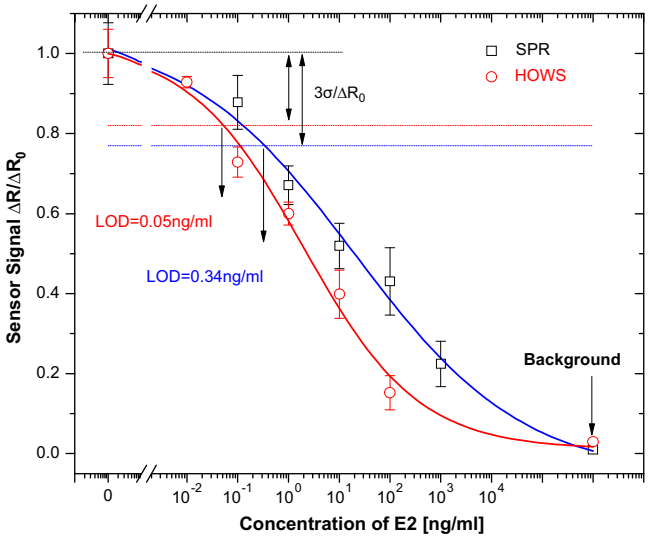

Fig. 5. Calibration curves for the detection of E2 measured by HOWS (circle) and SPR (square).

on the BSA-E2 conjugate attached to the flexible hydrogel polymer chains (which reduces the steric hindrance with respect to the crowded thiol SAM). Compared to the performance of other SPR biosensors for the detection of estradiol in buffer solution (LOD between 0.6 and 1.5 ng/ml [4,34]) and seawater/serum (LOD of 0.455 ng/ml [35]), the presented HOWS detection scheme offers about one order of magnitude higher sensitivity for the detection of E2. The study of the unspecific sorption to PNIPAAm hydrogel showed a negligible signal for artificial urine and indicated that for the analysis of a serum the net charge of the polymer networks should be further optimized.

4. Conclusions

A novel biosensor based hydrogel optical waveguide spectroscopy (HOWS) and an inhibition immunoassay was developed for the sensitive detection of E2 at concentrations as low as 50 pg/ml. The biosensor takes advantage of a large figure of merit enabling accurate measurement of binding-induced refractive index changes, high binding capacity, accessibility of binding sites attached to flexible polymer chains, and good anti-fouling properties. The limit of detection of presented HOWS was impeded by the slow diffusion of the large antibody against target analyte through the hydrogel matrix. Future research will be devoted to the implementation of HOWS for direct detection of low molecular weight molecules such as estradiol. We expect that HOWS is an excellently suited platform for direct detection of such analytes owing to fast diffusion of analyte through the hydrogel matrix, advanced binding capacity, large figure of merit, and the compatibility with existing SPR biosensor instruments.

Acknowledgment

This research was supported by the National Natural Science Foundation of China (No. 20771015), the National "111" Project of China's Higher Education (No. B07012) and the European Soft Matter Infrastructure project (ESMI), FP7-INFRASTRUCTURES-2010-1, Grant Agreement Number 262348 of the European Commission.

References

[1] J. Homola, S.S. Yee, G. Gauglitz, Sensor. Actuat. B-Chem 54 (1999) 3–15.
[2] B. Liedberg, C. Nylander, I. Lundstrom, Biosens. Bioelectron. 10 (1995) i–ix.
[3] J. Homola, Anal. Bioanal. Chem. 377 (2003) 528–539.
[4] D. Habauzit, J. Armengaud, B. Roig, J. Chopineau, Anal. Bioanal. Chem. 390 (2008) 873–883.
[5] J. Homola, Chem. Rev. 108 (2008) 462–493.
[6] X.D. Hoa, A.G. Kirk, M. Tabrizian, Biosens. Bioelectron. 23 (2007) 151–160.
[7] K.S. Phillips, Q. Cheng, Anal. Bioanal. Chem. 387 (2007) 1831–1840.
[8] Y. Arima, M. Toda, H. Iwata, Adv. Drug Deliv. Rev. 63 (2011) 988–999.
[9] P.W. Beines, I. Klosterkamp, B. Menges, U. Jonas, W. Knoll, Langmuir 23 (2007) 2231–2238.
[10] M.J.N. Junk, R. Berger, U. Jonas, Langmuir 26 (2010) 7262–7269.
[11] A. Aulasevich, R.F. Roskamp, U. Jonas, B. Menges, J. Dostalek, W. Knoll, Macromol. Rapid Commun. 30 (2009) 872–877.
[12] Y. Wang, C.J. Huang, U. Jonas, T.X. Wei, J. Dostalek, W. Knoll, Biosens. Bioelectron. 25 (2010) 1663–1668.
[13] Y.C. Wang, P. Su, X.X. Zhang, W.B. Chang, Anal. Chem. 73 (2001) 5616–5619.
[14] T.B. Xin, H. Chen, Z. Lin, S.X. Liang, J.M. Lin, Talanta 82 (2010) 1472–1477.
[15] R.G. Struble, B.P. Nathan, C. Cady, X. Cheng, M. McAsey, Exp. Gerontol. 42 (2007) 54–63.
[16] S. Wang, S. Lin, L. Du, H. Zhuang, Anal. Bioanal. Chem. 384 (2006) 1186–1190.
[17] D.M. Leech, M.T. Snyder, R.G. Wetzel, Sci. Total Environ. 407 (2009) 2087–2092.
[18] T.B. Xin, X. Wang, H. Jin, S.X. Liang, J.M. Lin, Z.J. Li, Appl. Biochem. Biotechnol. 158 (2009) 582–594.
[19] Y. Yoon, P. Westerhoff, S.A. Snyder, M. Esparza, Water Res. 37 (2003) 3530–3537.
[20] N. Yildirim, F. Long, C. Gao, M. He, H.C. Shi, A.Z. Gu, Environ. Sci. Technol. 46 (2012) 3288–3294.
[21] M.M. Sun, L.Y. Du, S.Q. Gao, Y.H. Bao, S.H. Wang, Steroids 75 (2010) 400–403.
[22] S. Zhu, Q. Zhang, L.H. Guo, Anal. Chim. Acta. 624 (2008) 141–146.
[23] Q. Xiao, H.F. Li, G.M. Hu, H.R. Wang, Z.J. Li, J.M. Lin, Clin. Biochem. 42 (2009) 1461–1467.
[24] E.A. Shirtcliff, D.A. Granger, E.B. Schwartz, M.J. Curran, A. Booth, W.H. Overman, Horm. Behav. 38 (2000) 137–147.
[25] C.J. Munro, G.H. Stabenfeldt, J.R. Cragun, L.A. Addiego, J.W. Overstreet, B.L. Lasley, Clin. Chem. 37 (1991) 838–844.
[26] K. Kuningas, T. Ukonaho, H. Pakkila, T. Rantanen, J. Rosenberg, T. Lovgren, T. Soukka, Anal. Chem. 78 (2006) 4690–4696.
[27] T. Kokko, L. Kokko, T. Lovgren, T. Soukka, Anal. Chem. 79 (2007) 5935–5940.
[28] R.J. Santen, L. Demers, S. Ohorodnik, J. Settlage, P. Langecker, D. Blanchett, P.E. Goss, S. Wang, Steroids 72 (2007) 666–671.
[29] K.R. Gee, E.A. Archer, H.C. Kang, Tetrahedron Lett. 40 (1999) 1471–1474.
[30] I. Anac, A. Aulasevich, M.J.N. Junk, P. Jakubowicz, R.F. Roskamp, B. Menges, U. Jonas, W. Knoll, Macromol. Chem. Phys. 211 (2010) 1018–1025.
[31] S. Chutipongtanate, V. Thongboonkerd, Anal. Biochem. 402 (2010) 110–112.
[32] M.J.N. Junk, U. Jonas, D. Hinderberger, Small 4 (2008) 1485–1493.
[33] G.E. Perlmann, L.G. Longsworth, J. Am. Chem. Soc. 70 (1948) 2719–2724.
[34] M. Miyashita, T. Shimada, H. Miyagawa, M. Akamatsu, Anal. Bioanal. Chem. 381 (2005) 667–673.
[35] H.C. Ou, Z.F. Luo, H. Jiang, H.M. Zhou, X.P. Wang, C.X. Song, Anal. Lett. 42 (2009) 2758–2773.